THE JOURNAL OF PHYSICAL CHEMISTRY B

Article

pubs.acs.org/JPCB

Lipid-Modified Polyethylenimine-Mediated DNA Attraction Evaluated by Molecular Dynamics Simulations

Sampada Bagai, Chongbo Sun, and Tian Tang*

Department of Mechanical Engineering, University of Alberta, Edmonton, Alberta, Canada T6G 2G8

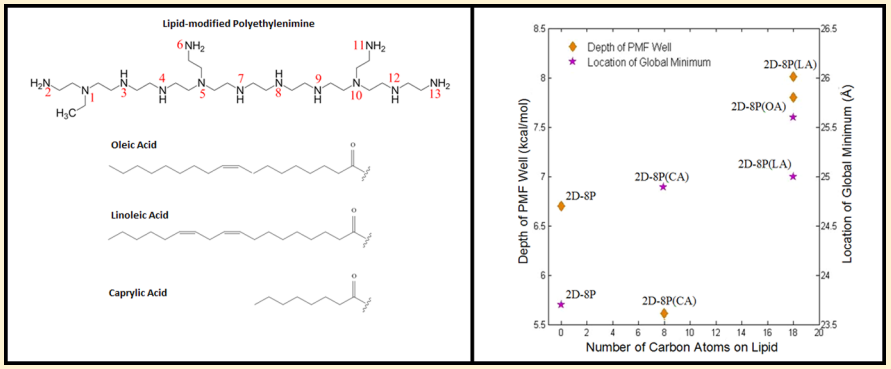

ABSTRACT: The effect of lipid modification on polyethylenimine (PEI)-mediated DNA attraction was studied by performing umbrella sampling molecular dynamics simulations that involved PEIs modified with three different types of lipids: oleic acid (OA), linoleic acid (LA), and caprylic acid (CA). The potential of mean force between two DNA molecules in the presence of these lipid-modified PEIs was calculated using the weighted histogram analysis method, and it predicted the stability and size of the DNA aggregate. When compared to native PEI, lipid modification was found to enhance the stability of DNA aggregation in the case of long lipids (LA and OA) but reduce the stability in the case of a short lipid (CA). In addition, LA-substituted PEI was shown to form stronger DNA aggregate than OA-substituted PEI, which correlates positively with previous experimental observations.

1. INTRODUCTION

Gene therapy offers a potential treatment for cancer and other hereditary diseases.[1] It requires the condensation (in the case of long molecules) or aggregation (in the case of short molecules) of nucleic acids into compact forms in order to facilitate their delivery into the target cells.[2,3] In vitro, it has been observed through various experimental settings that multivalent and polycationic ions are able to compact nucleic acid molecules into nanoparticles of approximately 300−400 nm diameter,[4−6] which bear the potential to serve as nonviral gene-delivery carriers. The efficacy of polycation-based gene-delivery carriers strongly depends on their molecular parameters, such as the molecular weight, structure, protonation state, and chemical modifications. For example, it has been found experimentally that substituting polycations with lipids increases their transfection efficiency.[7,8] Khalil et al.[9] studied the cellular uptake and transfection efficiency of DNA condensed by peptides substituted with stearyl moiety. They observed more stable complexes with the substitution, leading to higher cellular uptake. Incani et al.[10] substituted 25 kDa poly(L-lysine) (PLL) with different lipids. Compared to native PLL, the lipid-modified PLL provided better DNA protection and higher delivery efficiency. Bahadur et al.[11] substituted polyethylenimine (PEI) with palmitic acid and observed that the lipid substitution increased the zeta potential of DNA condensates. Chen et al.[12] studied DNA delivery mediated by 1800 Da PEI substituted with lauric acid and thioctic acid and found that the substitution increased the transfection efficiency to a level comparable to that of native 25 kDa PEI. Neanmark et al.[13] compared the transfection efficiency of 2 kDa PEI substituted with various lipids and observed that even one lipid substitution on each 2 kDa PEI could make it as efficient as native 25 kDa PEI, but without the high toxicity associated with the high-molecular-weight PEI.

Efforts have been spent on explaining the mechanisms behind the beneficial effect of lipid substitution. Hsu et al.[14] focused on the transfection pathways used by the delivery vectors and suggested that the reason for the increased cellular uptake of lipid-modified PEIs was the difference between their transfection pathways and those used by native PEIs. Specifically, low-molecular-weight native PEIs generally use caveolin-mediated endocytosis and macropinocytosis, whereas lipid-modified PEI may bring about additional pathways such as clathrin-mediated endocytosis. In a recent work, Sun et al.[15] used molecular dynamics (MD) simulations to study the effect of lipid substitution on DNA aggregation by PEIs. They observed that, compared to native PEIs, which aggregated DNA via electrostatic screening and polyion bridging (a polyion

Received: April 6, 2014
Revised: May 28, 2014
Published: June 11, 2014

   dx.doi.org/10.1021/jp503381r | J. Phys. Chem. B 2014, 118, 7070−7076

simultaneously attached to multiple DNAs),[16] lipid-modified PEIs aggregated DNA via a third mechanism: lipid association. Such association resulted in more water release from the solutes upon aggregation, which can potentially lead to more stable aggregates compared to those formed by native PEIs.[15] Posocco et al.,[17] via coarse-grained simulations, studied DNA binding with dendrons functionalized with cholesterol. Self-assembly of the hydrophobic units was observed, which was considered to be an important mechanism favoring the aggregation of DNA.

Although this self-assembly or lipid association facilitates aggregation, there are some drawbacks for the same. Sun et al.[15] observed that while lipid substitution promoted DNA aggregation through lipid association, it also hindered polyion bridging to some extent. Hence, the stability of the DNA aggregation is dependent on the delicate balance between the two mechanisms.[17] The steric hindrance brought about by the lipids can also influence the aggregation of DNAs. Experiments by Patel et al.[18] on spermine- and lipospermine-DNA binding suggested that the steric hindrance of the lipids did not allow lipospermine to induce compact toroidal DNA structures. Sun et al.[19] reported that increasing the lipid substitution levels on PEI (number of lipids per PEI) has a beneficial effect on the aggregation of nucleic acids when the lipid is short while it can have a reverse effect when the lipid is long. This was attributed to the association of lipid tails on individual PEIs and the steric hindrance resulting from the association. Due to the complex role lipid substitution may play in polycation-mediated DNA condensation or aggregation, the quantification of DNA attraction in the presence of lipid-modified polycations is in demand, which to the best of our knowledge is still absent in the literature.

In this work, we quantitatively studied the attraction of two DNA molecules in the presence of lipid-modified PEI molecules by calculating the potential of mean force (PMF) using umbrella sampling (US) MD simulations[20] coupled with the weighted histogram analysis method (WHAM).[21] A 586 Da branched PEI molecule is used as the native model, and it is modified with three different lipids, namely, oleic acid (OA), linoleic acid (LA), and caprylic acid (CA). For each type of PEI, the PMF of DNA attraction is obtained as a function of the reaction coordinate, which is the distance between the centers of mass of the two DNAs. Comparison among the PMF curves allows us to examine the size and stability of the formed aggregates quantitatively and address their dependence on the different lipid modifications.

The remainder of the article is organized as follows. In section 2, we describe the simulated systems, the US simulation details, and the WHAM analysis. Simulation results and discussion are presented in section 3. Conclusions are given in section 4.

2. METHOD

2.1. Simulated Systems. The DNA molecule used in this study is a Dickerson-Drew B-DNA dodecamer,[22] which has 24 nucleotides with the sequence d(CGCGAATTCGCG)^2. Each DNA carries a total charge of −22 in its fully deprotonated state. The PEIs simulated here are based on a model that has 13 amine groups with a molecular weight of 586 Da;[23] its molecular structure is shown in Figure 1. A protonation ratio of 46% is chosen, which is the reported protonation ratio for 600 Da PEI at pH 6.[24] This corresponds to 6 out of the 13 amine groups being protonated. The charges are distributed nearly

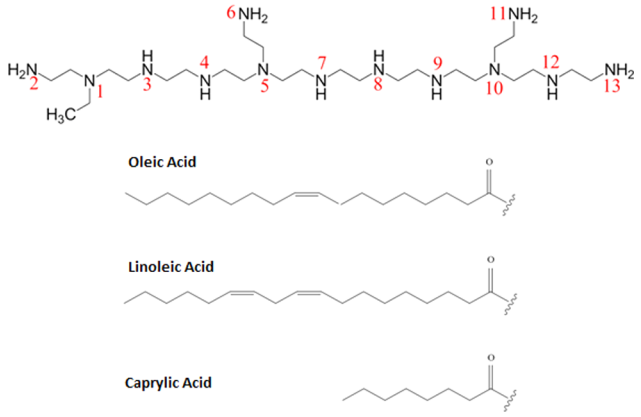

Figure 1. Molecular structure of the PEI-simulated and chemical structures of oleic acid, linoleic acid, and caprylic acid. The nitrogen numbers are given in red. Nitrogens 2, 4, 7, 9, 11, and 13 are protonated, giving a 46% protonation ratio, and lipids are substituted on nitrogen 6.

uniformly along the PEI, as shown in Figure 1. On the basis of this PEI, three lipid modifications are introduced, with OA, LA, and CA, respectively. Among these three lipids, OA and LA are longer (with 18 carbon atoms) and CA is shorter (with 8 carbon atoms). OA and LA have the same number of carbon atoms and a similar structure except for the presence of an extra double bond in LA. Each lipid tail is grafted onto a primary amine of the PEI (nitrogen number 6 in Figure 1), which does not affect the protonation ratio of the PEI

Three systems were simulated, each containing two DNAs and eight PEIs of a particular type as specified above. Throughout the article they are referred to as systems 2D-8P(OA), 2D-8P(LA), and 2D-8P(CA), respectively. Since in each system the total negative charge from the two DNA molecules was −44 while each PEI carried a charge of +6, the eight PEIs were not only able to neutralize the negative charges of DNA but also led to an N/P charge ratio (total PEI charges divided by total DNA charges) of >1, which was shown earlier to introduce stable DNA aggregates.[16] In the beginning of the simulations, each system had an initial configuration as shown in Figure 2, where the principle axes of DNAs and the axes of PEIs were aligned parallel to one another. Two PEIs were placed between the two DNAs such that their centers of mass (COMs) were equidistant from the COMs of the two DNAs. The rest of them were placed around the DNAs with their COMs at a distance of 20 Å from the COM of the nearest DNA molecule. Each system was placed in a water box sufficiently large that the distance between each DNA and the closest DNA in the periodic boxes is 72 Å. The net charge of +4 created by the two DNAs and eight PEIs was neutralized by adding four chlorine ions to the box, which is done by randomly replacing four water molecules. No additional salt ions were introduced. These three systems, together with a system containing two DNAs and eight native PEIs (named the 2D-8P system),[20] are compared in order to address the effect of different lipid substitutions on the DNA attraction.

2.2. WHAM Analysis. WHAM analysis together with US MD simulations was performed to extract the PMF for the DNA attraction. The distance between the COMs of the two DNAs was chosen as the reaction coordinate x. For each of the three systems described above, 29 US simulations were performed, and in each US simulation, the COMs of the

dx.doi.org/10.1021/jp503381r | J. Phys. Chem. B 2014, 118, 7070−7076

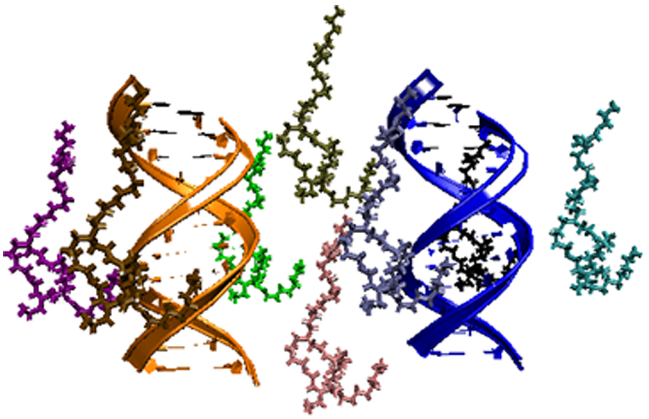

Figure 2. Initial configuration of the simulated systems. The PEIs shown here are substituted with OA, but the other two systems have the same initial configuration. In each US simulation, the COM separation between the two DNAs is adjusted according to the biasing potential, with the positions of the PEIs relative to the DNAs remaining the same. Water and ions are removed for clarity.

DNAs were subjected to a biasing potential in the form of $k((x - \alpha_i)/2)^2/2$ (i = 1, 2, ... 29). Here k is the force constant with a value of 2.0 kcal/mol/Å^2[25,26] and α_i is the equilibrium separation associated with the ith biasing potential. α_i has 29 values ranging from 22 to 50 Å at an interval of 1 Å. This selection was based on our previous work in which this amount of data was shown to generate sufficient sampling.[27] The entire range of the reaction coordinate was divided into bins. The size of the bin was assigned to be 0.25 Å, which was determined from a convergence test for the dependence of the PMF on the bin size. The data obtained from all 29 simulations were used to construct histograms which plotted the number of counts in each bin vs the reaction coordinate. The probability P_j^0 for the unbiased system (without the biasing potential applied at the DNA COMs) can then be obtained from the histograms, along with the free-energy shift ΔF_i for each US simulation. The two quantities are related by the WHAM equations as given below:[21]

$$P_j^0 = \frac{\sum_{i=1}^{s} n_i(x_j)}{\sum_{i=1}^{s} N_i e^{-\beta U_{\text{bias},i}(x_j)} e^{-\beta \Delta F_i}} \quad (1)$$

$$\Delta F_i = -\frac{1}{\beta} \ln\left\{ \sum_{j=1}^{m} P_j^0 e^{-\beta U_{\text{bias}}(x_j)} \right\} \quad (2)$$

$$U_{\text{bias},i}(x_j) = 2 \times \frac{1}{2} k \left(\frac{x_j - \alpha_i}{2} \right)^2 \quad (3)$$

In these equations, s = 29 is the total number of US simulations, m represents the total number of bins, N_i gives the total number of counts in the ith simulation, and $n_i(x_j)$ is the number of counts in the ith simulation that fall into the bin centered at x_j. $\beta = 1/k_B T$, where k_B is the Boltzmann constant and T is the temperature. The biasing potential $U_{\text{bias},i}(x_j)$ as given in eq 3 is twice the harmonic potential applied to each DNA since both DNAs are subjected to the same harmonic restraint. A MATLAB code was developed to solve the above equations iteratively to a satisfactory convergence, after which the PMF $W(x_j)$ was calculated using

$$W(x_j) = -k_B T \ln P_j^0(x_j) \quad (4)$$

The datum of the PMF was adjusted such that it became zero at a sufficiently large COM separation.

2.3. Simulation Details. As explained above, a total of 29 × 3 = 87 US simulations were performed. For all the simulations, the same procedure was followed, as explained below. The MD package NAMD[28] was used to perform the simulations, and VMD[29] was used for visualization and analysis of the trajectories. A CHARMM general force field[30] was used for the PEIs, and a CHARMM 27 force field[31] was used for the rest of the molecules. The TIP3P water model,[32] full electrostatics treated by the particle mesh Ewald method,[33] periodic boundary condition, the SHAKE algorithm[34] to constrain the hydrogen bonds, and a time step of 2 fs were used. The nonbonded interactions, including van der Waals and electrostatic forces, were cut off at 12 Å. In order to eliminate bad contact, each system was first minimized for 2000 steps with their solute molecules constrained. It was then minimized with harmonically restrained solutes for 2000 steps followed by 1000 steps of nonrestrained minimization. After the minimization, each system was gradually heated from 0 to 300 K in 20 ps, and the simulation was run for 4 ns at 300 K and 1 bar of pressure with harmonic restraint (constant = 10 kcal/mol/Å^2) applied to the nonhydrogen atoms of the solutes in order to relax the ions and water molecules surrounding the solutes. The restraint was then removed, and the systems were simulated under the isothermal−isobaric condition at 300 K and 1 bar. Each US simulation was run for 30 ns, and the data from the last 10 ns was used for analysis. Considering the 87 US simulations, the total simulation time in this work has exceeded 2.6 μs.

To assist in the discussion on the results from the US simulations, we also performed one unrestrained simulation for each of the three systems, where the biasing potential on the DNA COMs was absent. In these unrestrained simulations, the two DNAs were initially separated at a distance of 45 Å and then were allowed to move freely. Keeping all the other parameters the same as above, each unrestrained simulation was run for 200 ns to allow the system to reach equilibrium.

3. RESULTS AND DISCUSSION

As described above, 29 simulations were run for every system, with each simulation having a different harmonic restraint applied at the DNA COMs and a different initial COM separation distance. Due to the interaction between the two DNAs, the COM separation varies with simulation time, an example of which is shown in Figure 3. In this simulation, the two DNAs interact in the presence of eight OA-modified PEIs. The initial COM distance is 28 Å, which is also the distance at which the springs in the harmonic restraint are unstretched. For the first 4 ns (from −4 to 0 ns in Figure 3), a harmonic restraint was applied to all non-hydrogen atoms of the solutes to relax water and ions; hence the COM distance remains at 28 Å. When the restraint is removed at 0 ns (except the harmonic restraint applied at the COMs), the two DNAs first experience a repulsion due to the negative charges on them, leading to the rapid increase in the COM distance to 30 Å. As the PEI molecules equilibrate themselves around the DNAs and introduce an attractive interaction, the COM distance decreases and finally fluctuates at around 27.5 Å. This implies that when the harmonic restraint is applied at 28 Å, the interaction between the DNAs is attractive, and the equilibrium separation in the absence of the restraint should be less than 28 Å. A

dx.doi.org/10.1021/jp503381r | J. Phys. Chem. B 2014, 118, 7070−7076

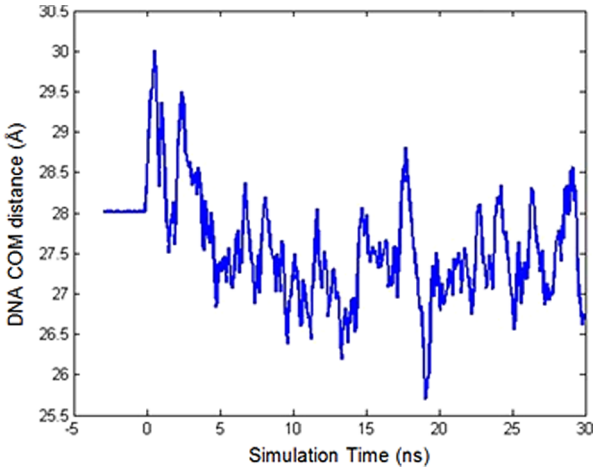

Figure 3. Example showing the variation of DNA COM distance with simulation time. Data were from one US simulation for system 2D-8P(OA), where the initial DNA COM distance was 28 Å.

histogram can be generated from this plot, and data from the 29 simulations were used to construct a plot that contains all of the histograms (Figure 4). In Figure 4, each curve represents data

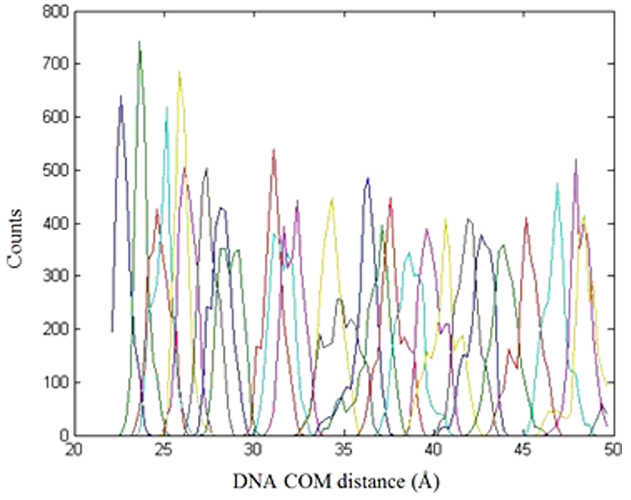

Figure 4. Histograms for the 2D-8P(OA) system showing the number of counts for the entire range of the reaction coordinates. A total of 29 US simulations were performed to generate the histograms. Different curves correspond to simulations with different biasing potential $U_{bias,i}$ (i = 1, 2,..., 29).

from one US simulation; together they show the number of counts for the entire range of the reaction coordinate. It is clear from Figure 4 that with the 29 simulations the histograms are well overlapped and good sampling is achieved. Using WHAM eqs 1−4, we can then generate the PMF curve from the histograms.

The PMF for system 2D-8P(OA) was plotted along the reaction coordinate in Figure 5a. The curve has three distinct regimes: the first from 22 to 25.6 Å which exhibits a decreasing trend and hence a repulsive interaction, the second from 25.6 to 44 Å which shows an increasing trend and attractive interaction, and the last beyond 44 Å which fluctuates without significant changes, indicating a negligible interaction. The distance 25.6 Å locates the global minimum in the PMF. It separates the repulsive and attractive branches and is the

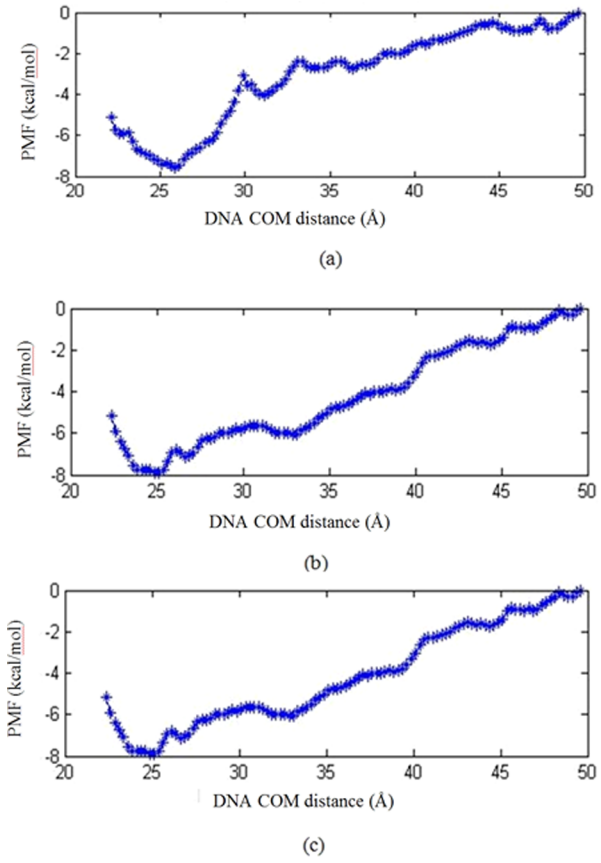

Figure 5. PMF vs DNA COM distance for systems (a) 2D-8P(OA), (b) 2D-8P(LA), and (c) 2D-8P(CA).

distance at which the two DNAs are neither repulsive nor attractive. In other words, this is the equilibrium separation between the DNAs and represents the size of the aggregate. The PMF value at the equilibrium separation, −7.8 kcal/mol in this case, is in magnitude equal to the energy required to dissociate the aggregate. Consequently, the depth of the PMF well is a quantitative description of the stability of the aggregate. Out of various factors that affect gene delivery, the size and stability of the formed condensates/aggregates are extremely important.[35] Therefore, the two quantities, equilibrium separation and depth of the PMF well, will be used to discuss the effectiveness of DNA aggregation mediated by lipid-modified PEIs.

The PMF curves for systems 2D-8P(LA) and 2D-8P(CA) are shown in Figure 5b,c, respectively. Qualitatively, these curves demonstrate similar characteristics to those for system 2D-8P(OA) with a similar amplitude of fluctuation, but the equilibrium separation and depth of the PMF well are different. Specifically, for system 2D-8P(LA), the PMF curve reaches its global minimum at 24.9 Å with a value of −8 kcal/mol. For system 2D-8P(CA), the curve reaches its global minimum at 25 Å, with a PMF value of −5.6 kcal/mol. These data are compared with the results for native PEI-mediated DNA attraction (system 2D-8P)[27] in Figure 6. It can be clearly seen that upon lipid substitution the equilibrium separation increases, suggesting an increase in the size of the DNA aggregate. The increase is 1.2 to 2 Å depending on the type of lipid: a longer lipid in general leads to a larger equilibrium separation. This can be attributed to the increased size of the PEI due to lipid substitution and the steric hindrances

dx.doi.org/10.1021/jp503381r | J. Phys. Chem. B 2014, 118, 7070−7076

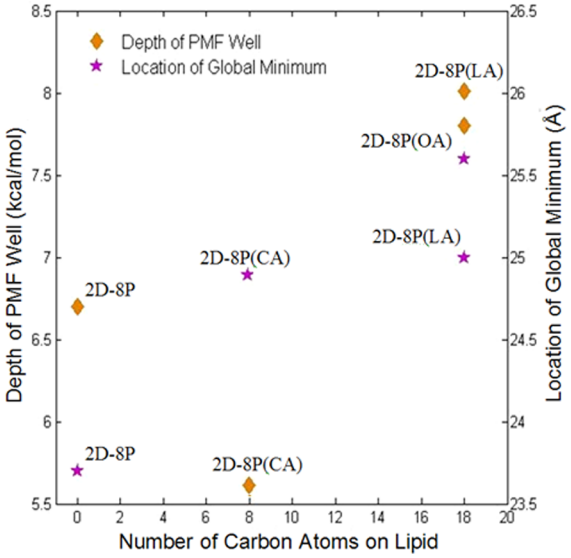

Figure 6. Equilibrium separation (location of global minimum) between the DNAs and depth of the PMF well for lipid-substituted and native PEI-mediated DNA attraction.

introduced by the lipids, which resist the formation of compact structures.[18]

When the depth of the PMF well is examined in Figure 6, it is seen that as compared to native PEI, for substitutions with long lipids (LA and OA) the depth of the PMF well has increased by 16−20%, whereas for a short lipid (CA) it has decreased by 17%. This indicates that despite the larger size, DNA aggregates formed by OA- and LA-substituted PEIs are more stable than native PEI-aggregated DNAs. On the other hand, the DNA aggregate mediated by CA-substituted PEI is not only larger but also less stable. A possible explanation for this can be provided by considering the mechanisms governing PEI-mediated DNA aggregation. Apart from charge neutralization, polycations also aggregate DNAs via polyion bridging, which is a reason that DNA aggregation mediated by polycations is more stable compared to small multivalent ions.[20] When lipid substitution is present, a third aggregation mechanism is introduced, namely, the association among the lipids on the PEIs attached to different DNAs.[5] Because the charges on the native PEI and the three lipid-modified PEIs are the same, the effect of charge neutralization is expected to be the same for all four systems. While lipid association is expected to add stability to the aggregation, the steric hindrance caused by the existence of lipids, on the other hand, can reduce the degree of polyion bridging[15,11] and weaken the DNA aggregation. For long lipids such as OA and LA, the lipid association can be sufficiently large to overcome the adverse effect on DNA aggregation caused by steric hindrance and less formation of polyion bridging, resulting in more stable aggregates when compared to the native PEI. On the other hand, a short lipid such as CA has a relatively small degree of lipid association, which may not be able to compensate for the decrease in attraction arising from less polyion bridging.[19]

Another interesting observation from Figure 6 is that LA- and OA-substituted PEIs, being very similar in structure, demonstrated different abilities to aggregate DNAs. The equilibrium DNA separation in the case of LA-modified PEIs is much smaller than the separation in the case of OA-modified PEIs and is comparable to the separation in the presence of short CA-modified PEIs. Meanwhile, LA-modified PEIs give rise to a greater PMF well depth than OA-modified PEIs. Therefore, among the three lipid-modified PEIs, LA-substituted PEI appears to provide the best balance between compactness and stability of the DNA aggregate. It can then be speculated that the degree of lipid association is the largest for LA and that the associations are most tightly formed.

To confirm this conjecture by quantifying the amount of lipid association, we performed unrestrained simulations for all three systems. These systems will be referred to as unrestrained 2D-8P(OA), 2D-8P(LA), and 2D-8P(CA). To determine the amount of lipid association, each system was simulated for 200 ns and data from the last 100 ns were used to compute the average. In the calculation, we consider every pair of lipid tails in a given system and determine how many pairs of carbon atoms on this pair of lipid tails are separated by 5 Å or less. If two carbon atoms are within 5 Å apart, then they will be called a bound pair. A distance 5 Å was used because it was shown to be the closest carbon atom separation when there is a favorable association between two alkane molecules.[36] Lipids OA and LA each have 18 carbon atoms. This means that there are 18 × 18 = 324 pairs of carbon atoms for a given pair of lipid tails. Out of these 324 pairs of carbons, the numbers of bound pairs are listed in Figure 7a,b. Similarly, CA has 8 carbon atoms and

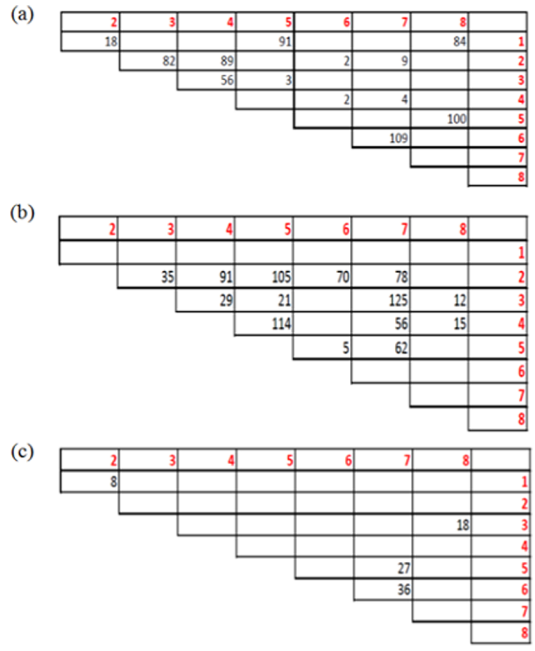

Figure 7. Number of pairs of carbon atoms between each pair of lipid tails that are closer than 5 Å in the unrestrained systems: (a) 2D-8P (OA), (b) 2D-8P (LA), and (c) 2D-8P (CA).

there are 8 × 8 = 64 pairs of carbons for a given pair of lipid tails. Figure 7c gives the numbers of bound pairs out of the 64 pairs. For each subfigure, the numbers in red are the indices for the eight lipid-modified PEIs. Each vacant cell indicates that there is no association between the pair of lipid tails in the given time frame. For example, the lipid on the first LA-substituted PEI (indexed as 1 in Figure 7b) is not associated with any other LA-substituted PEIs. For system 2D-8P(CA), there are only 4 nonempty cells, respectively corresponding to 8 bound pairs of lipid carbons between PEIs 1 and 2, 18 bound pairs between PEIs 3 and 8, 27 bound pairs between PEIs 5 and

dx.doi.org/10.1021/jp503381r | J. Phys. Chem. B 2014, 118, 7070−7076

7, and 36 bound pairs between PEIs 6 and 7. In addition, there is no mutual association among more than two PEI lipids. Compared to 2D-8P(CA), 2D-8P(OA) and 2D-8P(LA) have many more nonempty cells (13 for 2D-8P(OA) and 14 for 2D-8P(LA)), and the majority of these nonempty cells have numbers larger than 50. This implies a much more significant lipid association in these two systems, especially mutual associations among multiple lipids. Enhanced stability can be expected from the large lipid associations, which is consistent with their much larger PMF well depth as shown in Figure 6. Comparing systems 2D-8P(OA) and 2D-8P(LA), the main difference is the generally larger numbers in the nonempty cells of 2D-8P(LA). For a pair of lipid tails, the larger the number of bound carbon pairs, the tighter the association. Although the number of nonempty cells for 2D-8P(OA), 13, is comparable to the number of nonempty cells for 2D-8P(LA), 14, the total number of bound carbon pairs is 818 for 2D-8P(LA), a 26% increase from that for 2D-8P(OA), 649. This is in agreement with the PMF calculations where the DNA aggregate formed by LA-substituted PEIs is predicted to be not only more compact but also more stable compared to the DNA aggregate formed by OA-substituted PEIs.

It is of interest to compare our results with experimental observations in the literature. In an experimental study by Neamnark et al.,[13] the effect of different lipid substitutions on the cellular uptake and transfection efficiency of PEI-mediated gene delivery was studied. CA was found to be less effective in both cellular uptake and transfection as compared to other lipids. This is consistent with the largest and least-stable aggregate CA-substituted PEIs formed among the three lipid modifications. In addition, Neanmark et al.[13] reported that compared to OA, LA-substituted PEIs were more effective in cellular uptake and showed higher transfection efficiency during gene delivery. Hochgraf et al.[37] suggested that LA had a tendency to lower the crystallinity of the cell membrane. Roach et al.[38] studied the effect of different fatty acids on membrane properties and found that LA could reduce the membrane's phase-transition temperature. Both effects might increase the rate of motion of the molecules that have to move across the membrane and hence promote cellular uptake.[13] Despite these experimental studies, it was not clear whether there was a fundamental difference between the DNA aggregates formed by OA-substituted PEIs and those formed by LA-substituted PEIs. While our simulations here do not directly address the interaction of the aggregates with cell membrane or their uptake, it is encouraging to see that LA-substituted PEIs were able to form more lipid association and more compact DNA aggregates compared to OA, which correlates positively with the better uptake and transfection achieved with LA in experiments.

Recently, there was simulation work performed by Sun et al.,[19] where the effect of different lipid substitutions was studied on PEI-mediated siRNA (small-interfering RNA) complexation. They simulated LA- and CA-substituted PEI-mediated siRNA aggregation without applying any restraints to the molecules. Each lipid was substituted at two levels: one per PEI and three per PEI. Each simulated system involved 4 siRNAs and 18 lipid-modified PEIs, and for each system (a particular type of substitution at a particular substitution level), one unrestrained simulation was performed for a long time (200 ns). Compared to Sun's work, this work shows a few similarities but also some differences. Specifically, they observed that as the length of the lipid increases (from CA to LA), siRNA aggregates became more stable. This is consistent with our US MD results on the depth of the PMF wells. On the other hand, it was reported that siRNA aggregates mediated by lipid-modified PEIs, whether the substitution was by LA or CA, were more compact and stable than that by native PEIs. In the present work, CA-substituted PEIs were not able to form more compact or stable aggregates, and all aggregates formed by lipid-modified PEIs are larger than that formed by native PEIs. Several factors can contribute to such a difference. First, the native PEI in this work based on which the lipid modification is introduced is around 600 Da while the native PEI in ref 19 is around 2 kDa. The impact of lipid substitution on nucleic acid aggregation may be stronger for larger PEIs. Second, the aggregates formed in ref 19 involve more molecules (4 siRNAs and 18 PEIs). Although compared to native PEIs CA-substituted PEIs cannot form more stable aggregate for two DNAs, when they collectively aggregate more DNAs and form a network where all of the DNAs are mutually connected, the effect of lipid association can become more pronounced and hence the stability of the aggregate may be enhanced. For the same reason, when multiple DNAs are involved, the size of the aggregate may not necessarily increase with increasing length of the lipid as seen in the present work. It should be noted that the stability of the aggregate in ref 19 was assessed by examining the fluctuation in the radius of gyration of the siRNA aggregates, which was not as quantitative as the depth of PMF used in the present work. Therefore, although our US MD simulation involving two DNAs has its limitation in mimicking the aggregation process, it possesses the important advantage of providing a quantitative measure of the strength of aggregation. It should be favorable to explore the PMF for the aggregation of multiple nucleic acid molecules. However, defining PMF for more than two DNAs or RNAs is challenging since it is not clear what would be the best choice for the reaction coordinate.

4. CONCLUSIONS

The effect of lipid substitution on PEI-mediated DNA attraction was studied using US MD simulations coupled with WHAM. PMF was calculated for the interaction between two DNA molecules in the presence of PEIs modified with three types of lipids—OA, CA, and LA—where the center-to-center distance between the two DNAs served as the reaction coordinate. Compared to native PEIs, all three lipid-substituted PEIs gave rise to less compact DNA aggregates. In addition, PEIs substituted with short lipid (CA) formed less-stable DNA aggregates than native PEIs. PEIs substituted with long lipids (OA and LA), on the other hand, enhanced the stability of the DNA aggregates. The observed behavior was attributed to the competition between steric hindrance brought about by the lipids, which increases the size and decreases the stability of the aggregate, and the hydrophobic association among the lipids, which promotes aggregation and enhances the stability. Unrestrained MD simulations confirmed that among the three lipids LA has the largest amount of association, which agrees with the PMF data as well as past experimental observations.

AUTHOR INFORMATION

Corresponding Author

*Tel: (780) 492-5467. E-mail: tian.tang@ualberta.ca.

Notes

The authors declare no competing financial interest.

■ ACKNOWLEDGMENTS

We acknowledge the computing resources and technical support from Compute Canada and the high performance computing facility at the National Institute for Nanotechnology, Edmonton, Canada. This work was supported by the Natural Science and Engineering Research Council of Canada, Alberta Innovates − Technology Futures, and the Canada Foundation for Innovation.

■ REFERENCES

(1) Ledley, F. D. Non-viral Gene Therapies: The Promise of Genes as Pharmaceutical Products. *Hum. Gene Ther.* **1995**, *6*, 1129−1144.
(2) Christiano, R.; Curiel, D. Strategies to accomplish Gene Delivery via the Receptor-mediated Endocytosis Pathway. *Cancer Gene Ther.* **1996**, *3*, 49−57.
(3) Phillips, S. Receptor-mediated DNA Delivery Approaches to Human Gene Therapy. *Biologicals* **1995**, *23*, 13−16.
(4) Gosule, L.; Schellman. Compact form of DNA induced by Spermidine. *J. Nat.* **1976**, *259*, 333−335.
(5) Shirts, M.; Mobley, D.; Chodera. Alchemical Free Energy Calculations. Ready for Prime Time ? *J. Annu. Rep. Comput. Chem.* **2007**, *3*, 41−59.
(6) Hansma, H.; Golan, R.; Hsieh, W.; Lollo, C.; Mullen-Ley, P.; Kwoh, D. DNA Condensation for Gene Therapy as Monitored by Atomic Force Microscopy. *Nucleic Acids Res.* **1998**, *26*, 2481−2487.
(7) Incani, V.; Lavasanifar, A.; Uludağ, H. Hydrophobic Modification of Cationic Polymers on route to Superior Gene Carriers. *Soft Matter* **2010**, *6*, 2124−2138.
(8) Navarro, G.; Sawant, R. R.; Biswas, S.; Essex, S.; Ilarduya, C.; Torchilin, V. P-glycoprotein Silencing with siRNA Delivered by DOPE-modified PEI overcomes Doxorubicin Resistance in Breast Cancer Cells. *Nanomedicine* **2012**, *7*, 65−78.
(9) Khalil, I.; Futaki, S.; Niwa, M.; Baba, Y.; Kaji, N.; Kamiya, H. Mechanism of Imrpoved Gene Transfer by the N-terminal Stearylation of Octaarginine: Enhanced Cellular Association by Hydrophobic Core Formation. *Gene Ther.* **2004**, *11*, 636−644.
(10) Incani, V.; Lin, X.; Lavasanifar, A.; Uludağ, H. Relationship between the Extent of Lipid Substitution on Poly(L-Lysine) and DNA Delivery Efficiency. *ACS Appl. Mater. Interfaces* **2009**, *1*, 841−848.
(11) Bahadur, K. C. R.; Landry, B.; Aliabadi, H. M.; Lavasanifar, A.; Uludag, H. Lipid-substitution on Low Molecular Weight (0.6 - 2.0 kDa) Polyethylenimine leads to Higher Zeta-potential with Plasmid DNA and enhances Transgene Expression. *Acta Biomater.* **2011**, *7*, 2209−2217.
(12) Chen, X.; Yuan, Z.; Yi, X.; Zhuo, R.; Li, F. Crosslinked Self-assemblies of Lipoid acid-substituted Low Molecular Weight (1800 Da) Polyethylenimine as Reductive−sensitive Non-viral Gene Vectors. *Nanotechnology* **2012**, *23*, 415602.
(13) Neamnark, A.; Suwantong, O.; Bahadur, R. K. C.; Hsu, C. Y. M.; Supaphol, P.; Uludag, H. Aliphatic Lipid Substitution on 2 kDa-polyethylenimine improves Plasmid Delivery and Transgene Expression. *Mol. Pharmaceutics* **2009**, *6*, 1798−1815.
(14) Hsu, C.; Uludağ, H. A Simple and Rapid Nonviral Approach to efficiently Transfect Primary Tissue−derived Cells using Polyethylenimine. *Biomaterials* **2012**, *33*, 7834−7848.
(15) Sun, C.; Tang, T.; Uludağ, H. Probing the Effects of Lipid Substitution on Polycation Mediated DNA Aggregation: A Molecular Dynamics Simulations Study. *Biomacromolecules* **2012**, *13*, 2982−2988.
(16) Sun, C.; Tang, T.; Uludağ, H. Molecular Dynamics Simulations of PEI Mediated DNA Aggregation. *Biomacromolecules* **2011**, *12*, 3698−3707.
(17) Posocco, P.; Pricl, S.; Jones, S.; Barnard, A.; Smith, D. K. Less is More − Multiscale Modelling of Self-assembling Multivalency and its Impact on DNA Binding and Gene Delivery. *Chem. Sci.* **2010**, *1*, 393−404.
(18) Patel, M.; Anchordoquy, T. Contribution of Hydrophobicity to Thermodynamics of Ligand-DNA Binding and DNA Collapse. *Biophys. J.* **2005**, *88*, 2089−2103.
(19) Sun, C.; Tang, T.; Uludag, H. A Molecular Dynamics Simulation Study on the effect of Lipid Substitution on Polyethylenimine Mediated siRNA Complexation. *Biomaterials* **2013**, *34*, 2822−2833.
(20) Bagai, S.; Sun, C.; Tang, T. Potential of Mean Force of Polyethylenimine Mediated DNA Attraction. *J. Phys. Chem. B* **2013**, *117*, 49−56.
(21) Kumar, S.; Rosenberg, J. M.; Bouzida, D.; Swendsen, R. H.; Kollman, P. A. The Weighted Histogram Analysis Method for Free-energy Calculations on Biomolecules. I. The Method. *J. Comput. Chem.* **1992**, *13*, 1011−1021.
(22) Tereshko, V.; Minasov, G.; Egli, M. The Dickerson-Drew B-DNA Dodecamer Revisited at Atomic Resolution. *J. Am. Chem. Soc.* **1999**, *121*, 470−471.
(23) Sun, C.; Tang, T.; Uludağ, H.; Cuervo, J. Molecular Dynamics Simulations of DNA/PEI Complexes: Effect of PEI Branching and Protonation State. *Biophys. J.* **2011**, *100*, 2754−2763.
(24) Utsuno, K.; Uludag, H. Thermodynamics of PEI-DNA Binding and DNA Condensation. *Biophys. J.* **2010**, *99*, 201−207.
(25) Dai, L.; Mu, Y.; Nordenskiold, L.; Maarel, J. R. C. Molecular Dynamics Simulation of Multivalent-ion Mediated Attraction between DNA Molecules. *Phys. Rev. Lett.* **2008**, *100*, 118301−118304.
(26) Khalid, S.; Bond, P.; Holyoake, J.; Hawtin, R.; Sansom, M. DNA and Lipid Bilayers: Self-assembly and Insertion.? *J. R. Soc. Interfaces* **2008**, *5*, 241−250.
(27) Bagai, S.; Sun, C.; Tang, T. Potential of Mean Force of Polyethylenimine-Mediated DNA Attraction. *J. Phys. Chem. B* **2013**, *117*, 49−56.
(28) Phillips, J.; Braun, R.; Wang, W.; Gumbart, J.; Tajkhorshid, E.; Villa, E.; Chipot, C.; Skeel, R.; Kale, L.; Schulten, K. Scalable Molecular Dynamics with NAMD. *J. Comput. Chem.* **2005**, *26*, 1781−1802.
(29) Humphrey, W.; Dalke, A.; Schulten, K. VMD: Visual Molecular Dynamics. *J. Mol. Graphics* **1996**, *14*, 33−38.
(30) Vanommeslaeghe, K.; Hatcher, E.; Acharya, C.; Kundu, S.; Zhong, S.; Shim, J.; Darian, E.; Guvench, O.; Lopes, P.; Vorobyov, I. M. A. CHARMM General Force Field: A Force Field for Drug-like Molecules Compatible with the CHARMM all-atom Additive Biological Force Fields. *J. Comput. Chem.* **2010**, *31*, 671−690.
(31) MacKerel, A., Jr.; Brooks, C., III; Nilsson, L.; Roux, B.; Won, Y. In *The Encyclopedia of Computational Chemistry*; John Wiley & Sons: Chichester, U.K., 1998; Vol. *1*, pp 271−277.
(32) Jorgensen, W. L. Transferable Intermolecular Potential Functions for Water, Alcohols, and Ethers. Application to Liquid Water. *J. Am. Chem. Soc.* **1981**, *103*, 335−340.
(33) Darden, T.; York, D.; Pedersen, L. Particle Mesh Ewald − an N.log(N) method for Ewald Sums in Large Systems. *J. Chem. Phys.* **1993**, *98*, 10089−10092.
(34) Ryckaert, J.; Ciccotti, G.; Berendsen, H. Numerical Integration of the Cartesian Equations of Motion of a System with Constraints: Molecular Dynamics of *n*-alkanes. *J. Comput. Phys.* **1977**, *23*, 327−341.
(35) Abbasi, M.; Uludag, H.; Incani, V.; Hsu, C.; Jeffery, A. Further Investigation of Lipid-substituted Poly(L-Lysine) Polymers for Transfection of Human CRL Fibroblasts. *Biomacromolecules* **2008**, *9*, 1618−1630.
(36) Thomas, A. S.; Elcock, A. H. Direct Measurement of the Kinetics and Thermodynamics of Association of Hydrophobic Molecules from Molecular Dynamics Simulations. *J. Phys. Chem. Lett.* **2011**, *2*, 19−24.
(37) Hochgraf, E.; Mokady, S.; Cogan, U. Dietary Oxidized Linoleic Acid Modifies Lipid Composition of Rat Liver Microsomes and Increases Their Fluidity. *J. Nutr.* **1997**, *127*, 681−686.
(38) Roach, C.; Feller, S. E.; Ward, J. A.; Shaikh, S. R.; Zerouga, M.; Stillwell, W. Comparison of cis and trans Fatty Acid containing Phosphatidylcholines on Membrane Properties. *Biochemistry* **2004**, *43*, 6344−6351.